Chem. Senses 33: 425–432, 2008

doi:10.1093/chemse/bjn009
Advance Access publication March 3, 2008

Effect of Superoxide Derived from Lucifer Yellow CH on Voltage-Gated Currents of Mouse Taste Bud Cells

Keita Takeuchi and Kiyonori Yoshii

Graduate school of Life Science and Systems Engineering, Kyushu Institute of Technology, Hibikino 2-4, Kitakyushu 808-0196, Japan

Correspondence to be sent to: Kiyonori Yoshii, Graduate School of Life Science and Systems Engineering, Kyushu Institute of Technology, Hibikino 2-4, Kitakyushu 808-0196, Japan. e-mail: yoshii@brain.kyutech.ac.jp

Abstract

Lucifer yellow CH (LY), a fluorescent membrane-impermeable cell marker dye, has been routinely loaded into cells through recording electrodes to visualize these cells after electrophysiological investigation, without considering its pharmacological effect. Recently, we showed that the exposure of cells loaded with LY to light for microscopy produced unidentified radical species that retarded the inactivation of voltage-gated Na^+ currents irreversibly (Higure Y et al. 2003). Here, we show that superoxide dismutase, an enzyme that decomposes superoxide, reverses the retardation effect, which assures that superoxide is the unidentified radical species. The estimated mean lifetime of superoxide in recording electrodes (in the absence of cytoplasm) is approximately 6 min, and hence, the Na^+ currents are retarded even in the dark, when LY is exposed to light before being loaded into the cell. Superoxide has no effect on voltage-gated Cl^- currents. These results show that superoxide action on ion channels is rather selective. The breakdown of superoxide inside cells and the effect of endogenous superoxide on the superoxide-susceptible channels are discussed.

Key words: sodium currents, superoxide dismutase, whole-cell recording

Introduction

Superoxide is a by-product of aerobic metabolism and a starting material for peroxynitrite and other reactive oxygen species such as hydrogen peroxide and hydroxyl radical. Because of their high chemical reactivity, these radical species have been suggested to cause a variety of diseases and physiological damage, including cancer (Oberley and Buettner 1979; Totter 1980), inflammation (McCord 1974; Guzik et al. 2003), and possibly aging (Beckman and Ames 1998; Alexeyev et al. 2004; Hussain and Mitra 2004). In molecular levels, reactive oxygen species (Duprat et al. 1995; Tokube et al. 1996; Sobey et al. 1997) and peroxynitrite (Brzezinska et al. 2000) modify a variety of K^+ channels and the L-type Ca^{2+} channel (Tokube et al. 1996), and hydrogen peroxide modifies voltage-gated sodium channels (Wang GK and Wang SY 2002). However, the effect of superoxide on voltage-gated Na^+ channel remains unknown.

Lucifer yellow CH (LY), a fluorescent membrane-impermeable cell marker dye, has been routinely loaded into cells through intracellular recording electrodes to visualize these cells after electrophysiological investigation, without considering its pharmacological effect. Although a recording electrode with a fine tip barely leaks LY without motive power, that with a large tip such as a patch pipette for whole-cell clamping leaks LY into cells during the electrophysiological study. In a previous study, we showed that halogen light illumination (at ordinary intensities for microscopy) of cells loaded with LY produced a radical species and that the radical species caused decreased inactivation of tetrodotoxin (TTX)-sensitive, voltage-gated Na^+ channel by increasing the mean open time of the channel (Higure et al. 2003). However, the radical species remained to be identified. In this paper, we identify the radical species, investigate its effect on other voltage-gated currents, and discuss the mechanism of the effect.

Materials and methods

All experimental protocols were conducted in compliance with the Guiding Principles for the Care and Use of Animals in the Field of Physiological Sciences approved by the Council of the Physiological Society of Japan.

Peeled lingual epithelium

Peeled lingual epithelia containing taste buds were prepared as described previously (Furue and Yoshii 1997, 1998). In brief, ddY-strain mice (5–8 weeks) were anesthetized with ether and then decapitated to remove their tongues, which were incubated in Earle's solution for approximately 10 min with 95% O_2 / 5% CO_2 bubbling at 25 °C after the subcutaneous injection of an elastase solution (the chemical composition of this and other solutions are shown in Solution section). The epithelia were peeled with taste buds intact, then mounted on a recording platform with the trans side (taste pore side) down, and placed under a differential interference contrast microscope (BX50; Olympus, Tokyo, Japan) equipped with a 60× water-immersion objective (Figure 1).

The taste pore side, facing inside the recording platform, was always immersed in a physiological saline. The cis side, the exposed basolateral membrane of taste bud cells, was irrigated with the physiological saline or a dithiothreitol (DTT) solution.

Electrophysiology

Voltage-clamp currents of ion channels were investigated with patch clamping techniques (Higure et al. 2003). In brief, the recording electrode was placed on the basolateral membrane of a taste bud cell under visual guidance. The Na^+ current was investigated with a Cs^+ electrode solution, and the tip potential of approximately −7 mV was neglected. The tetraethylammonium (TEA)-sensitive outward rectifier K^+ current, the inward rectifier K^+ current, and the Cl^- current were examined with a K^+-gluconate electrode solution, and the tip potential of approximately −15 mV was compensated by subtracting −15 mV from a series of command potentials. The resistance of recording electrodes was approximately 5 MΩ irrespective of their electrode solutions.

Voltage-gated currents generated by a series of test potentials from a holding potential of −70 mV were recorded with an amplifier (Axopatch 200B; Axon Instruments, Union City, CA), filtered at 10 kHz, digitized with an analogue-to-digital converter (Digidata 1322A, Axon Instruments), and stored using pCLAMP data acquisition software (version 8.2, Axon Instruments) on a personal computer. We averaged the magnitude of voltage-gated currents over the last 5 ms and took the average as that of a steady-state current.

A TTX solution, TEA solution, a Cl^--free solution, and a DTT solution were bath applied and washed away with the physiological saline similarly applied. All experiments were carried out at room temperature.

Application of LY, newborn calf serum, and superoxide dismutase

Cells were loaded with LY via recording electrodes. The time constant of the diffusion of LY into cells depended on the resistance of the recording electrodes, for example, 52 s, 4.8 MΩ; 96 s, 6.0 MΩ; and 217 s, 8.9 MΩ. Because the resistance of recording electrodes used for quantitative measurements was less than 5 MΩ, and because we started electrophysiological recordings 2 min after rupturing patch membranes, the concentration of LY at channels examined was almost at a steady state (Figure 5). Newborn calf serum (final concentration of 0.05 ml/ml; COSMOBIO, Tokyo, Japan) and superoxide dismutase (SOD) (final concentration of 223.5 units/ml; Sigma, St Louis, MO; S2515, bovine erythrocyte) were similarly applied into cells via recording electrodes. The concentration of newborn calf blood serum

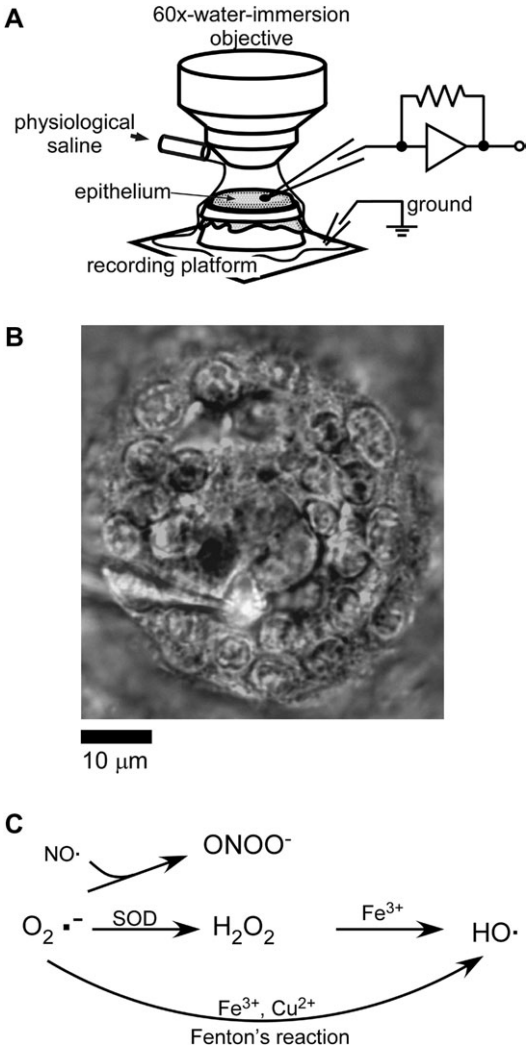

Figure 1 Experimental setup for taste bud cells **(A)** and a LY-loaded taste bud cell **(B)** and superoxide metabolites **(C)**. (A) A peeled lingual epithelium is mounted on a recording platform, placed under a 60× water-immersion objective, where the Na^+ current of taste bud cells is investigated under whole-cell clamp conditions. (B) Top view of a differential interference contrast image of a taste bud and a recording electrode overlaid on its fluorescence image. (C) Reactive oxygen species. Dots depict the unpaired electron. $O_2{\cdot}^-$, superoxide; NO·, nitric oxide; $ONOO^-$, peroxynitrite; H_2O_2, hydrogen peroxide; HO·, hydroxyl radical.

was typical of that in cell culture media, and that of SOD was the same as that in B-18, a serum-free medium.

Illumination

We used 3 types of illumination protocols, *L*0–*L*2, to typify scenarios used in patch clamp research (e.g., Figure 3A). *L*0 consisted of fluorescent room lighting of approximately 1.0×10^3 lx. *L*1 was the upward illumination of 5.0×10^3 lx from the condenser lens of the microscope. The direction and intensity of the *L*1 were usual for microscopy. *L*2 was the downward illumination of 5.0×10^3 lx at source, which was filtered between 400 and 440 nm with a dichroic mirror unit (U-MWIG; Olympus). The direction and the intensity of the *L*2 were usual for florescent microscopy.

Prior to experiments, LY was freshly dissolved in an electrode solution under *L*0 and was then kept in the dark on ice for more than 30 min to degrade the radical species produced during the illumination. The experimental protocol usually consisted of the following sequence: 1) *L*0 (20 s), during which time the recording electrode was loaded with an electrode solution and mounted on the micromanipulator; 2) *L*1 (40s), during which time the recording electrode was applied to a taste bud cell and a giga-ohm seal was established; and 3) *L*2, the duration of which was adjusted to suit the various experiments. In some experiments, *L*2 was interposed with dark periods of various durations or with the 40-s *L*1. The duration of the *L*0 and the *L*1 remained constant, even if the tasks were completed early. All cells examined were exposed to the 20-s *L*0 and the 40-s *L*1 before the onset of whole-cell clamping, unless otherwise noted.

Curve fittings

The time constants of the inactivating current ($\tau_{inactivation}$), the magnitude of the non-inactivating current (NIC), and the magnitude of the inactivating current extrapolated to the onset of depolarization (at $t = 0$) were estimated by fitting a single exponential curve to the data

$$y = a + b \cdot \exp\left(\frac{-t}{\tau}\right), \quad (1)$$

where a is the magnitude of the NIC at a steady state, b is that of the inactivating current at $t = 0$, and τ is $\tau_{inactivation}$ (Figure 2B). The Na^+ current fitted with this equation was elicited by a series of test potentials from a holding potential of −70 mV or by a test potential of −20 mV from the holding potential.

The time constants for the decrease of the $\tau_{inactivation}$, the $\tau_{inactivation}$ at a steady state, and the $\tau_{inactivation}$ at $t = 0$ were estimated by the same equation, where a is the $\tau_{inactivation}$ at

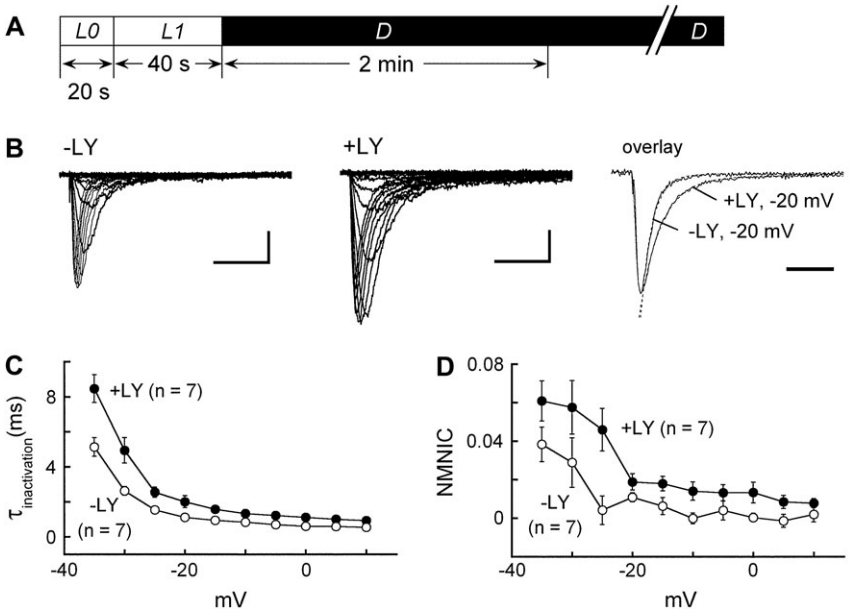

Figure 2 Retarded inactivation of TTX-sensitive, voltage-gated Na^+ currents in the dark. Taste bud cells were examined with the Cs^+ electrode solution. **(A)** Illumination protocol applied to the experiments shown in this figure. *L*0, a 20-s exposure to the room light, during which we filled a recording electrode with an electrode solution and set it on a micromanipulator. *L*1, a 40-s exposure to the upward illumination in a microscope, during which we guided a recording electrode on the basolateral membrane of a taste bud cell and formed a giga-ohm seal. In the dark (*D*), we ruptured the patch membrane, compensated voltage-clamp conditions, and started the recording of Na^+ currents 2 min after rupturing. **(B)** Traces of the Na^+ current family (see Electrophysiology section) obtained from a control cell (−LY), those of a LY-loaded cell (+LY), and curve-fitted traces taken one each from −LY and +LY (overlay). Traces shown were TTX-sensitive Na^+ currents in this and following figures. Overlaid traces were elicited by a depolarization to −20 mV, normalized to its peak in magnitude, and fitted with dotted lines drawn with single exponential curves (see Curve fittings section). Time scales, 5 ms for −LY and +LY and 2 ms for overlay. Current scales, 200 pA. **(C)** The $\tau_{inactivation}$ of control cells (open circles, mean ± SD, $n = 7$) and LY-loaded cells (closed circles, $n = 7$) as a function of membrane potential. **(D)** NMNIC, the ratio of NIC to the peak in magnitude, plotted similarly to (C).

the steady state, b is the $\tau_{inactivation}$ at $t = 0$, and τ is the time constant for the decrease of the $\tau_{inactivation}$ (Figure 4B). Similarly, the time constant for the decrease of the magnitude of normalized NIC (NMNIC, the ratio of NIC to the peak in magnitude), the normalized NIC at the steady state, and that at $t = 0$ were estimated, where a is the NMNIC at the steady state, b is the NMNIC at $t = 0$, and τ is the time constant for the decrease of the NMNIC (Figure 4C).

Solutions

All solutions were prepared with deionized water, and the components are expressed in millimolar concentrations, unless otherwise noted. The physiological saline comprised 150 NaCl, 5 KCl, 2 $CaCl_2$, 0.5 $MgCl_2$, 10 glucose, 5 HEPES, pH 7.4/NaOH. The TTX solution was prepared by adding 1 μM TTX to the physiological saline. The TEA solution was prepared by adding 10 mM TEA-Cl to the TTX solution. The Cl^--free solution was prepared by replacing 155 mM Cl^- in the TEA solution with equimolar methanesulfonate. The DTT solution was prepared by adding 1 mM DTT to the physiological saline. The elastase solution comprised 0.1% elastase (Wako Pure Chemical Industries, Osaka, Japan) dissolved in the physiological saline. The Cs^+ electrode solution comprised 120 CsCl, 15 NaCl, 5 $MgCl_2$, 10 EGTA, 5 Na_2ATP, 0.3 Na_3GTP, 10 HEPES, pH 7.2/CsOH. The K^+-gluconate electrode solution comprised 120 K-gluconate, 20 KCl, 2 $MgCl_2$, 10 EGTA, 2 Na_2ATP, 0.25 Na_3GTP, 10 HEPES, pH 7.2/KOH. The LY-loaded electrode solution was freshly prepared by adding the dilithium salt of LY (Sigma) to these electrode solutions to make a concentration of 4.2 mM, a usual concentration for marking cells.

Results

Retardation effects in the dark

Previously, exposure of LY-loaded taste bud cells to light retarded the inactivation of TTX-sensitive Na^+ currents, some of which became non-inactivated (Higure et al. 2003). In the present study, we found that the Na^+ current was similarly retarded in cells that were not exposed to light after loading with LY (Figure 2). Single exponential curves fitted the inactivating part of the Na^+ current with correlation coefficients >0.99. Both the time constant ($\tau_{inactivation}$) and the NMNIC (see Curve fittings section) thus obtained were significantly larger than those for control cells (cells investigated without LY) at all test potentials examined (2-way analysis of variance, $P < 0.05$). In the following study, we investigated the effect of LY on the Na^+ current elicited by depolarization from a holding potential of −70 mV to a test potential of −20 mV.

Preexposure effects

Normally, the LY-loaded electrode solution was exposed to fluorescent room light ($L0$) for 20 s and to upward illumination ($L1$) for 40 s, before the rupture of patch membranes. We tested whether the preexposure caused the retardation effect in the dark by giving another preexposure, $L2$, for different durations, T, up to 6 min (Figure 3A).

In control cells, the 6-min exposure to the $L2$ hardly increased the $\tau_{inactivation}$ and the NMNIC (Figure 3B). In cells loaded with LY, both the $\tau_{inactivation}$ and NMNIC increased with increasing T (Figure 3C). The 6-min $L2$ exposure significantly (t-test, $P < 0.05$) increased the $\tau_{inactivation}$ from 2.01 ± 0.31 ms (mean ± standard deviation [SD], $T = 0$, $n = 7$) to 3.95 ± 0.34 ms ($T = 6$, $n = 6$) and the NMNIC from 0.019 ± 0.0041 ($T = 0$, $n = 7$) to 0.075 ± 0.012 ($T = 6$, $n = 6$). Also, both $\tau_{inactivation}$ and NMNIC of LY-loaded cells had already become larger than those of control cells before

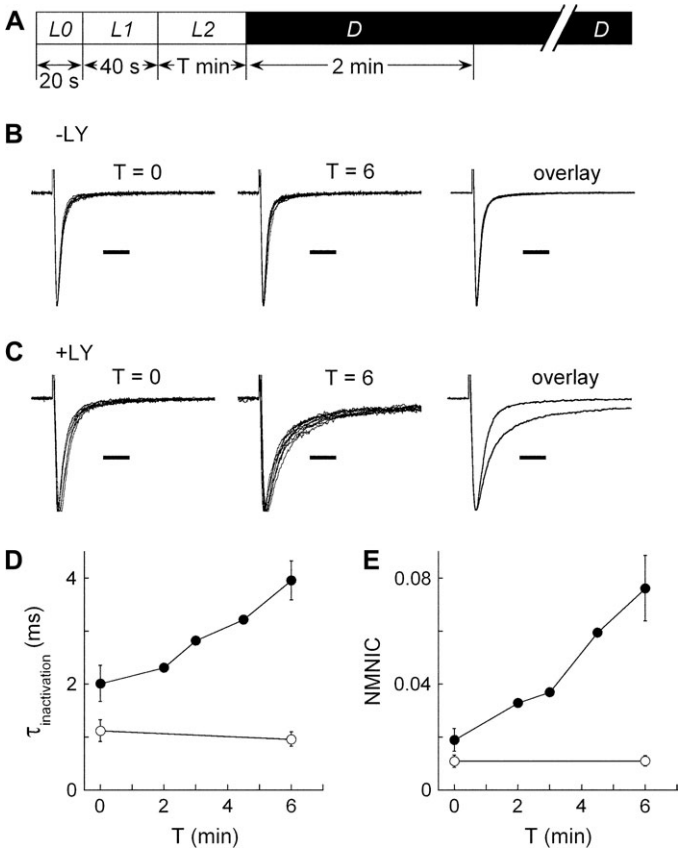

Figure 3 Retardation effect caused by preexposure of LY. Taste bud cells were examined with the Cs^+ electrode solution. **(A)** Illumination protocol applied to the experiments shown in this figure (see Illumination section). $L2$, an exposure to the downward illumination for a given period, T. **(B)** Overlaid traces of the Na^+ current of control cells (−LY) exposed to the 0-min $L2$ ($T = 0$, $n = 7$), the 6-min $L2$ ($T = 6$, $n = 6$), and the overlay of averaged traces shown in $T = 0$ and $T = 6$ (overlay). The Na^+ current was elicited on depolarization from a holding potential of −70 mV to a test potential of −20 mV in this and the following figures. Each trace was obtained from a different cell and is normalized to its peak in magnitude. **(C)** Traces obtained from LY-loaded cells (+LY) overlaid similarly to (B). **(D)** The $\tau_{inactivation}$ obtained from control cells (open circles) and LY-loaded cells (closed circles) as a function of T. **(E)** NMNIC plotted similarly to (D). Data plotted in (D) and (E) are mean ± SD ($n = 7$ at $T = 0$, $n = 6$ at $T = 6$) of their respective traces shown in (B) and (C), and the others are obtained from one cell each. Time scales, 5 ms.

the exposure to the *L*2 (*T* = 0 at Figures 3D and E). These results suggest that the radical species is produced by the pre-exposure in recording electrodes and survives until the injection. Also it is suggested that the same radical species is responsible for the retardation effect in light and in dark.

The application of the DTT solution blocked the retardation effect in the dark (data not shown). The $\tau_{inactivation}$ obtained from cells treated with the DTT solution and then loaded with LY was 1.18 ± 0.13 (*n* =3), and that from control cells treated with the DTT solution was 1.07 ± 0.07 (*n* = 3). There was no significant difference (*t*-test, $P > 0.05$). These results agreed with our previous study that DTT as a radical scavenger neutralized the retardation effect in light (Higure et al. 2003).

Time-dependent decrease of retardation effect

In order to estimate the lifetime of the radical species, we used the following light/dark exposure protocol (Figure 4). After exposure to a 20-s *L*0, we exposed the LY-loaded recording electrode to a 6-min *L*2, kept it standing in dark for a given time *T*, and then exposed it to a 40-s *L*1 to perform a whole-cell voltage-clamp. Note that one cell supplies only one point of data in the figure.

The $\tau_{inactivation}$ decreased with increasing *T* with a time constant of 7.4 min. The NMNIC similarly decreased with increasing *T*, with a time constant of 5.0 min. These long and reasonably similar time constants suggest that the lifetime of the radical species is sufficiently long to be nontrivial during neurophysiological experimentation. If the extent of the retardation effect varies linearly with concentration of the radical species, then the mean lifetime is equal to the time constant (5.0–7.4 min).

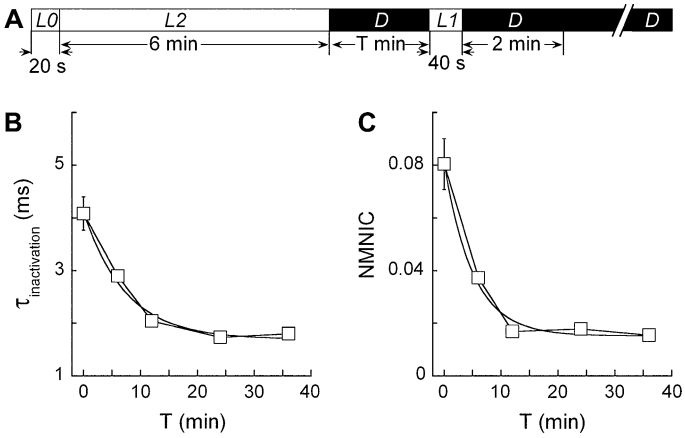

Figure 4 Time-dependent decrease of the retardation effect. Taste bud cells were examined with the Cs^+ electrode solution supplemented with LY. **(A)** Illumination protocol applied to the experiments shown in this figure. Notations are the same as in Figure 3A except that *L*2 period is fixed to 6 min; that the first dark period is variable, *T*; and that the recording of the Na^+ current for curve fitting starts 2 min after the onset of the second dark period. **(B)** The $\tau_{inactivation}$ as a function of *T*. **(C)** NMNIC as a function of *T*.

The estimated $\tau_{inactivation}$ at the steady state was 1.70 ms, which is close to the $\tau_{inactivation}$ of 2.11 ± 0.29 ms (*n* = 7) obtained from LY-loaded cells exposed to the 20-s *L*0 and the 40-s *L*1. Similarly, the estimated NMNIC at the steady state (0.015) was close to that obtained from cells exposed to the 20-s *L*0 and the 40-s *L*1 (0.017 ± 0.0037, *n* = 7). These results showed that the estimated $\tau_{inactivation}$ and NMNIC were close to those obtained with the exposure to the 40-s *L*1 alone. It suggests that the radical species produced by the 6-min *L*2 was decomposed completely with the time constant of 5.0–7.4 min during the dark period of approximately 30 min.

Effect of SOD

The above results showed that the radical species lived long when it was kept standing outside cells (Figure 4); the radical species produced by the *L*2 exposure was kept standing in the dark for *T* min in recording electrodes placed apart from cells and then applied inside cells to estimate the lifetime. If the radical species has the same lifetime inside cells, the retardation effect would keep developing for more than 5.0–7.4 min after turning off the illumination. However, the retardation effect stopped developing in approximately 1 min after turning off the illumination (Figures 5 and 6), which agreed with our previous results (Higure et al. 2003). These results showed that the radical species was short lived inside cells. It is likely that the lifetime depends on cytoplasm.

We thus investigated constituents of cytoplasm that inhibited the retardation effect. Initially, we added newborn calf serum, a constituent of cytoplasm, to LY-loaded recording electrodes. The addition suppressed the retardation effect on the $\tau_{inactivation}$ and the NMNIC under a periodic exposure to *L*2 (Figure 6). We then tested the effect of SOD, a cytoplasmic enzyme that selectively decomposes superoxide (McCord and Fridovich 1969; McCord 1974), under the same periodic exposure. The addition of SOD to the LY-loaded recording electrode completely blocked the retardation effect. When SOD was heated at 95 °C for 30 min to be inactivated, it failed to inhibit the retardation. These results suggest that the radical species that retards the inactivation is superoxide.

Effect of superoxide on action potentials and voltage-gated Cl^- currents

The action potentials of taste bud cells elongated after the exposure to *L*2 (Figure 7), suggesting that superoxide also modified outward rectifier currents that form action potentials together with the Na^+ current. We investigated the effect of superoxide on the voltage-gated Cl^- channel because our previous study showed that it generated outward currents on depolarization and hence formed the repolarizing phase of action potentials in a subtype of taste bud cells (Noguchi et al. 2003).

First, we confirmed our previous results. The addition of TEA slightly decreased outward current magnitude, and

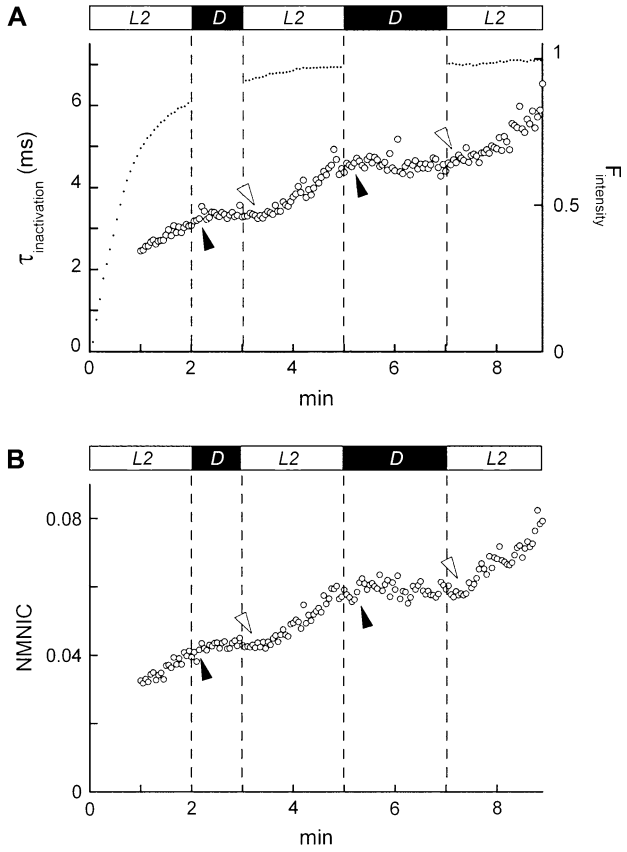

Figure 5 Illumination-dependent development of the retardation effect on a taste bud cell examined with the Cs^+ electrode solution supplemented with LY. All cells examined in this and following figures are exposed to a 20-s *L*0 and a 40-s *L*1 before the onset of whole-cell clamping, unless otherwise noted. The taste bud cell is then periodically exposed to *L*2 for indicated duration. We rupture the patch membrane to start whole-cell clamping and turn on the first *L*2 simultaneously. The recording of the TTX-sensitive Na^+ current for curve fitting starts 1 min after the rupture. **(A)** The $\tau_{inactivation}$ under periodic illumination as a function of time after the rupture. Dotted line, fluorescence intensity of LY ($F_{intensity}$) inside the cell calculated relative to the maximum one. Open arrowheads, the delay in starting the development of the retardation effect after turning on the illumination. Closed arrowheads, the delay in stopping the development of the retardation effect after turning off the illumination. **(B)** NMNIC as a function of time after the onset of recording. The notation of arrowheads is the same as in (A).

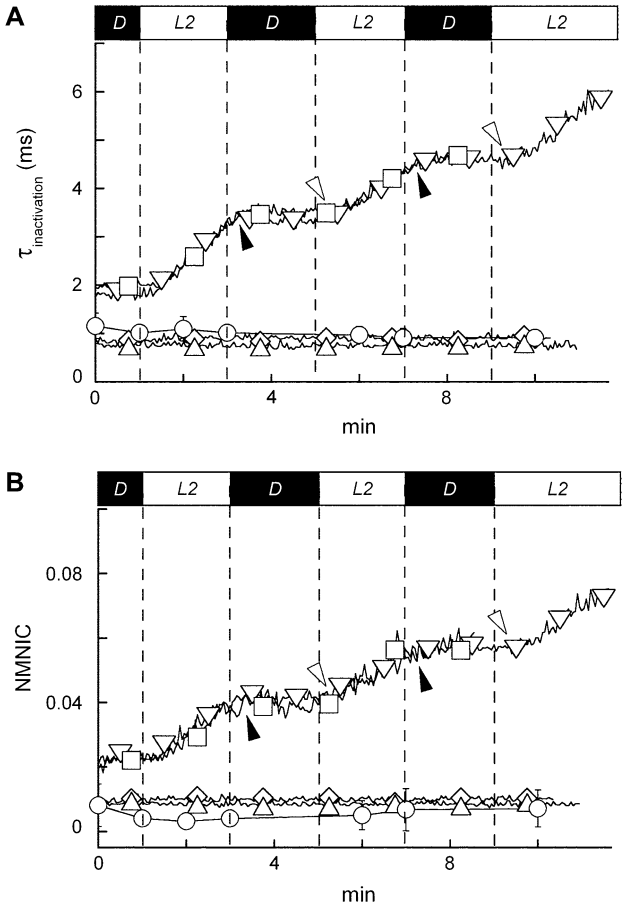

Figure 6 Block of the retardation effect by blood serum or SOD. Taste bud cells are periodically exposed to *L*2 for indicated duration. The recording of the TTX-sensitive Na^+ current for curve fitting starts 1 min after the onset of the first *D* and followed by periodic *L*2 illumination. **(A)** The $\tau_{inactivation}$ as a function of time after the onset of recording. **(B)** NMNIC plotted similar to (A). Taste bud cells were examined with Cs^+ electrode solution (circles) that supplemented with LY (squares), LY and bovine blood serum (triangles), LY and SOD (diamonds), and LY and heat inactivated SOD (inverted triangles). Each symbol except circles and inverted triangles plots one data point in every 30th, and the other data are plotted with dots. Each inverted triangles plots one data in every 20th. Circles plot all data. Notations of arrowheads in (A) and (B) are the same as in Figure 5A.

the replacement of Cl^- in the TEA solution with methanesulfonate caused the lost of the remaining current at all membrane potentials examined (Figure 8). These results showed that the primary outward current in the presence of 10 mM TEA was the voltage-gated Cl^- current. The Cl^- current was insensitive to superoxide. These results suggest that the modified Na^+ current solely elongated action potentials.

Discussion

The present results showed that the radical species that retarded the inactivation of the Na^+ current was superoxide and that superoxide survived in the absence of SOD and modified the Na^+ current even in the dark. These results warned that special care, typically the application of DTT or SOD to LY-loaded recording electrodes, is needed to eliminate artifacts caused by superoxide.

The elongation of action potentials by superoxide suggested that superoxide decreased the magnitude of ion currents needed for the repolarization phase of action potentials. However, voltage-gated Cl^- currents were insensitive to superoxide. Also, superoxide never decreased the magnitude of TEA-sensitive outward rectifier currents (data not shown). Rather, superoxide slightly increased their magnitude. Similarly, superoxide increased the magnitude of inward rectifier K^+ currents (data not shown), though it was not involved in the generation of action potentials. These results suggest that the modified Na^+ current solely

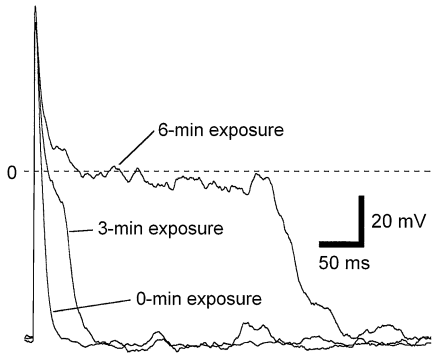

Figure 7 Action potentials of a taste bud cell widened by the retardation effect. The taste bud cell examined with the K^+-gluconate electrode solution supplemented with LY is exposed to *L2* for indicated duration. Action potentials are elicited by 1.0-ms current pulse of 200 pA from a holding current of −60 pA. A dashed line represents the 0-mV level.

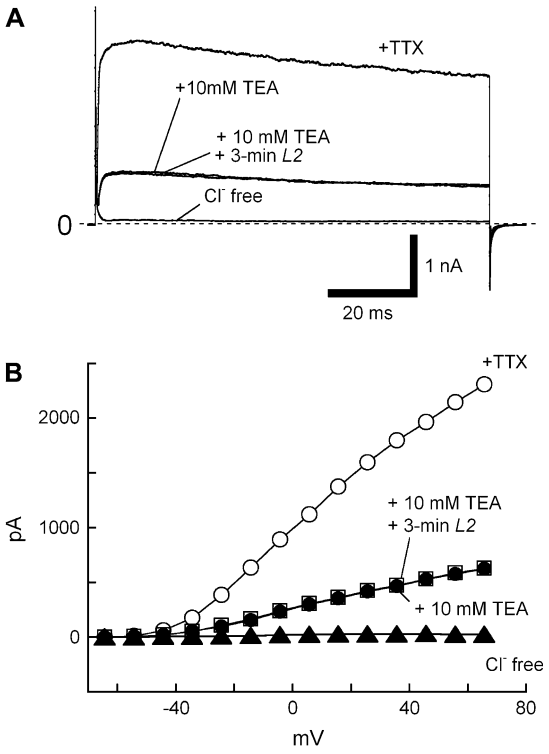

Figure 8 Effect of a 3-min *L2* on the Cl^- current of a taste bud cell examined with the LY-containing K^+-gluconate electrode solution. **(A)** Traces of membrane currents obtained from a cell. The currents were examined in the TTX solution (+TTX), in the TEA solution, after the exposure to the 3-min *L2* in the TEA solution, and in the Cl^--free solution (containing 10 mM TEA), in order. The membrane potential was depolarized from a holding potential of −85 mV to +65 mV. **(B)** Current–voltage relations of the same cell shown in (A). Holding potential, −85 mV.

elongated action potentials against the slight increase in the K^+ current that shortened the width of action potentials. Also, it is suggested that the LY effect selectively modifies voltage-gated channels.

Although superoxide is a starting material for hydrogen peroxide, hydroxyl radical, and peroxynitrite, it is unlikely that these reactive oxygen species except peroxynitrite are responsible for the modification of the Na^+ current as follows. Hydrogen peroxide did not contribute to the modification because SOD that inhibited the modification produced hydrogen peroxide. Neither did hydroxyl radical. Although hydroxyl radical is synthesized via Fenton's reaction, hydroxyl radical hardly occurs under the present experimental conditions because we added neither iron nor copper ions essential for the Fenton's reaction to the electrode solution. Peroxynitrite, an anion, may contribute to the modification because it may be synthesized with endogenous nitrogen oxide. However, the effect of peroxynitrite on the Na^+ current remains unknown, though it is shown that peroxynitrite inhibits amiloride-sensitive Na^+ channels in *Xenopus* oocytes (DuVall et al. 1998).

It is shown that predominant ultraviolet species in the earth atmosphere, UVA, hampers the gating of several Na^+ channels including Nav1.5, Nav1.4, and native Na^+ channels in rat GH_3 cells and that hydrogen peroxide applied outside cells similarly modifies Nav1.5 channel gating (Wang GK and Wang SY 2002). The discrepancy may result from the concentration of hydrogen peroxide used or the difference in the type of Na^+ channels examined. Hydrogen peroxide applied outside cells was as high as 1.5% in their study. If we produced a lot of superoxide molecules inside cells, applied SOD would produce more hydrogen peroxide molecules and modify the Na^+ current. Although Nav1.4 and probably native GH_3 Na^+ channels are TTX sensitive as similar to the Na^+ current we examined in this study, they may be minor components in mouse taste bud cells.

The mechanisms of how superoxide exerted its effects remained to be investigated. Because superoxide is a membrane-impermeable anion, it would remain inside cells and oxidize the superoxide-susceptible channels exposed to intracellular spaces. In the previous study, we suggested that unidentified radical species would oxidize cytoplasmic loop-linking homologous repeat domains III and IV of Na^+ channel proteins because it is shown that the modification of this region slows inactivation and prolongs channel open times (Stuhmer et al. 1989). Because the present study identified the radical species as superoxide, superoxide would oxidize the cytoplasmic loop. Also, superoxide may oxidize other parts that regulates the open and close of the susceptible channels to increase the mean open time of the channel because the outward rectifier K^+ current and the inward rectifier K^+ current are noninactivating.

The widening of action potentials may occur not only in taste bud cells but also in neurons. Although the SOD is ubiquitous, its mutation would cause the widening under physiopathological conditions because superoxide is a by-product of aerobic metabolism. The widened action potentials would increase neurotransmitter release at presynaptic membranes, increase the conduction velocity, and decrease

bursting frequencies. Oxygen-free radicals are related to aging (Beckman and Ames 1998; Alexeyev et al. 2004; Hussain and Mitra 2004), inflammation (McCord 1974; Guzik et al. 2003), and cancer (Oberley and Buettner 1979; Totter 1980). The modification of the Na^+ channel may be involved in these phenomena.

Shortly after turning off the illumination, further development of the retardation effect ceased (closed arrowheads in Figures 5 and 6). Although the production of superoxide de novo stopped in the dark, the LY-loaded recording electrode would supply superoxide to the cell continuously by diffusion. Cytosolic SOD also continuously escaped by diffusion into the recording electrode. However, Mn-SOD, a subtype of SOD in mitochondria (Steinman and Hill 1973) would remain inside cells and keep decomposing superoxide. The rapid termination of any further development suggests that the molecular activity of SOD is very fast. Actually, the molecular activity of SOD is as fast as that of catalase, an enzyme showing the fastest measured molecular activity.

When the illumination of LY-loaded cells was turned on, the retardation effect occurred with a short delay (open arrowheads in Figures 5 and 6) and developed in a steady rate. The short delay suggests that the concentration of superoxide is slowly increased after turning on the illumination. The steady rate suggests that the concentration reaches a steady level where the synthesis and decomposition are at equilibrium because the superoxide effect was irreversible.

Acknowledgements

21st Century COE program (center no. J19) granted to Kyushu Institute of Technology by MEXT of Japan.

References

Alexeyev MF, Ledoux SP, Wilson GL. 2004. Mitochondrial DNA and aging. Clin Sci (Lond). 107:355–364.

Beckman KB, Ames BN. 1998. The free radical theory of aging matures. Physiol Rev. 78:547–581.

Brzezinska AK, Gebremedhin D, Chilian WM, Kalyanaraman B, Elliott SJ. 2000. Peroxynitrite reversibly inhibits Ca(2+)-activated K(+) channels in rat cerebral artery smooth muscle cells. Am J Physiol Heart Circ Physiol. 278:H1883–H1890.

Duprat F, Guillemare E, Romey G, Fink M, Lesage F, Lazdunski M, Honore E. 1995. Susceptibility of cloned K^+ channels to reactive oxygen species. Proc Natl Acad Sci USA. 92:11796–11800.

DuVall MD, Zhu S, Fuller CM, Matalon S. 1998. Peroxynitrite inhibits amiloride-sensitive Na+ currents in Xenopus oocytes expressing alpha beta gamma-rENaC. Am J Physiol. 274:C1417–C1423.

Furue H, Yoshii K. 1997. In situ tight-seal recordings of taste substance-elicited action currents and voltage-gated Ba currents from single taste bud cells in the peeled epithelium of mouse tongue. Brain Res. 776: 133–139.

Furue H, Yoshii K. 1998. A method for in-situ tight-seal recordings from single taste bud cells of mice. J Neurosci Methods. 84:109–114.

Guzik TJ, Korbut R, Adamek-Guzik T. 2003. Nitric oxide and superoxide in inflammation and immune regulation. J Physiol Pharmacol. 54: 469–487.

Higure Y, Katayama Y, Takeuchi K, Ohtubo Y, Yoshii K. 2003. Lucifer Yellow slows voltage-gated Na+ current inactivation in a light-dependent manner in mice. J Physiol. 550:159–167.

Hussain AM, Mitra AK. 2004. Effect of reactive oxygen species on the metabolism of tryptophan in rat brain: influence of age. Mol Cell Biochem. 258:145–153.

McCord JM. 1974. Free radicals and inflammation: protection of synovial fluid by superoxide dismutase. Science. 185:529–531.

McCord JM, Fridovich I. 1969. Superoxide dismutase. An enzymic function for erythrocuprein (hemocuprein). J Biol Chem. 244:6049–6055.

Noguchi T, Ikeda Y, Miyajima M, Yoshii K. 2003. Voltage-gated channels involved in taste responses and characterizing taste bud cells in mouse soft palates. Brain Res. 982:241–259.

Oberley LW, Buettner GR. 1979. Role of superoxide dismutase in cancer: a review. Cancer Res. 39:1141–1149.

Sobey CG, Heistad DD, Faraci FM. 1997. Mechanisms of bradykinin-induced cerebral vasodilatation in rats. Evidence that reactive oxygen species activate K+ channels. Stroke. 28:2290–2294; discussion 2295.

Steinman HM, Hill RL. 1973. Sequence homologies among bacterial and mitochondrial superoxide dismutases. Proc Natl Acad Sci USA. 70: 3725–3729.

Stuhmer W, Conti F, Suzuki H, Wang XD, Noda M, Yahagi N, Kubo H, Numa S. 1989. Structural parts involved in activation and inactivation of the sodium channel. Nature. 339:597–603.

Tokube K, Kiyosue T, Arita M. 1996. Openings of cardiac KATP channel by oxygen free radicals produced by xanthine oxidase reaction. Am J Physiol. 271:H478–H489.

Totter JR. 1980. Spontaneous cancer and its possible relationship to oxygen metabolism. Proc Natl Acad Sci USA. 77:1763–1767.

Wang GK, Wang SY. 2002. Modifications of human cardiac sodium channel gating by UVA light. J Membr Biol. 189:153–165.

Accepted January 26, 2008